THE JOURNAL OF BIOLOGICAL CHEMISTRY VOL. 284, NO. 43, pp. 29968–29978, October 23, 2009
© 2009 by The American Society for Biochemistry and Molecular Biology, Inc. Printed in the U.S.A.

A Conserved Serine Residue Is Required for the Phosphatidate Phosphatase Activity but Not the Transcriptional Coactivator Functions of Lipin-1 and Lipin-2*

Received for publication, May 21, 2009, and in revised form, August 10, 2009 Published, JBC Papers in Press, August 28, 2009, DOI 10.1074/jbc.M109.023663

Jimmy Donkor[‡], Peixiang Zhang[‡], Samantha Wong[‡], Lauren O'Loughlin[‡], Jay Dewald[§], Bernard P.C. Kok[§1], David N. Brindley[§2], and Karen Reue[‡3]

From the [‡]Departments of Human Genetics and Medicine, David Geffen School of Medicine, UCLA, Los Angeles, California 90095 and the [§]Department of Biochemistry, Signal Transduction Research Group, University of Alberta, Edmonton, Alberta, T6G 252 Canada

Mammalian lipins (lipin-1, lipin-2, and lipin-3) are Mg^{2+}-dependent phosphatidate phosphatase (PAP) enzymes, which catalyze a key reaction in glycerolipid biosynthesis. Lipin-1 also functions as a transcriptional coactivator in conjunction with members of the peroxisome proliferator-activated receptor family. An S734L mutation in *LPIN2* causes Majeed syndrome, a human inflammatory disorder characterized by recurrent osteomyelitis, fever, dyserythropoietic anemia, and cutaneous inflammation. Here we demonstrate that mutation of the equivalent serine in mouse lipin-1 and lipin-2 to leucine or aspartate abolishes PAP activity but does not impair lipin association with microsomal membranes, the major site of glycerolipid synthesis. We also determined that lipin-2 has transcriptional coactivator activity for peroxisome proliferator-activated receptor-response elements similar to lipin-1 and that this activity is not affected by mutating the conserved serine. Therefore, our results indicate that the symptoms of the Majeed syndrome result from a loss of lipin-2 PAP activity. To characterize sites of lipin-2 action, we detected lipin-2 expression by *in situ* hybridization on whole mouse sections and by quantitative PCR of tissues relevant to Majeed syndrome. Lipin-2 was most prominently expressed in liver, where levels were much higher than lipin-1, and also in kidney, lung, gastrointestinal tract, and specific regions of the brain. Lipin-2 was also expressed in circulating red blood cells and sites of lymphopoiesis (bone marrow, thymus, and spleen). These results raise the possibility that the loss of lipin-2 PAP activity in erythrocytes and lymphocytes may contribute to the anemia and inflammation phenotypes observed in Majeed syndrome patients.

The mammalian lipin protein family is composed of three members, lipin-1, lipin-2, and lipin-3, each of which are ~100 kDa in size and have 44–48% amino acid similarity (reviewed in Ref. 1). Orthologous lipin genes are present in plants, invertebrates, and single cell eukaryotes such as yeast and plasmodium (2), suggesting that lipin proteins play a fundamental cellular role that has been conserved in evolution. In particular, extended stretches of 100–200 amino acids at the N-terminal and C-terminal regions of the protein (the N-LIP and C-LIP domains, respectively) are highly conserved among the three mammalian lipin family members and among species. Within the C-LIP domain are two key protein functional motifs as follows: a haloacid dehalogenase motif (D*X*D*X*T) found in a superfamily of Mg^{2+}-dependent phosphatases (3, 4), and a transcription factor-binding motif (L*XX*IL) (5). These motifs confer two distinct molecular functions on members of the lipin family. All three mammalian lipins are Mg^{2+}-dependent phosphatidate phosphatase (PAP)[4] enzymes, which catalyze the conversion of phosphatidate (PA) to diacylglycerol, a key step in the biosynthesis of triacylglycerol, phosphatidylcholine, and phosphatidylethanolamine (3, 4, 6, 7). Lipin-1 also acts as a transcriptional coactivator in hepatocytes, where it interacts with a complex containing peroxisome proliferator-activated receptor (PPAR) α and PPARγ coactivator-1α (PGC-1α) to regulate the expression of genes involved in fatty acid oxidation (5). Roles for lipin-2 and lipin-3 as transcriptional coactivators have not been characterized.

All three mammalian lipin family members function as PAP enzymes, raising the question of why multiple proteins are required. Previous gene expression studies in a panel of mouse and human tissues indicate that the three lipin genes have distinct but overlapping tissue distributions (6). Lipin-1 is most prominently expressed in adipose tissue, skeletal muscle, cardiac muscle, and testis, with lower expression in other tissues, including liver, kidney, and brain. Lipin-2 is expressed at high levels in liver and also to some extent in kidney, brain, and gut. Lipin-3 is expressed at much lower levels in the tissues surveyed, but mRNA is detectable in liver and gut. There is some overlap in the tissue expression of some lipin family members, making it unclear how each contributes to PAP and coactivator function. For example, lipin-1 and lipin-2 are both expressed in liver, although the relative levels and cell types in which they are

* This work was supported, in whole or in part, by National Institutes of Health Grants HL28481 and HL90553 (to K. R.) and S-T32-HG002536 (to J. D.). This work was also supported by Canadian Institute of Health Research Grant MOP 89726 (to D. N. B.).

[1] Recipient of a studentship award from the Muttart Diabetes Research and Training Centre.

[2] Medical Scientist for the Alberta Heritage Foundation for Medical Research.

[3] To whom correspondence should be addressed: Dept. of Human Genetics, Gonda 6506A, David Geffen School of Medicine, UCLA, 695 Charles E. Young Dr. South, Los Angeles, CA 90095. Fax: 310-794-5446; E-mail: reuek@ucla.edu.

[4] The abbreviations used are: PAP, Mg^{2+}-dependent phosphatidate phosphatase; PA, phosphatidate; PPARα, peroxisome proliferator-activated receptor-α; PGC-1α, PPARγ coactivator protein-1α; PPRE, PPAR-response element; qPCR, quantitative PCR; HAD, haloacid dehalogenase; f, forward; r, reverse.

expressed have not been definitively determined. Studies of PAP and coactivator activity in liver have thus far focused largely on lipin-1, which is required for normal induction of fasting-induced gene expression (5), and accounts for the glucocorticoid-regulated PAP activity in this tissue (8). However, recent work has also implicated lipin-2 as an important contributor to hepatic PAP activity, which is up-regulated in the liver of lipin-1-deficient mice, is induced by fasting, and is increased in obesity (9). In addition, studies employing RNA-mediated silencing of lipin-1 or lipin-2 in cultured HeLa M cells and 3T3-L1 cells indicate that lipin-1 and lipin-2 have distinct functions (10).

Further evidence that lipin-1 and lipin-2 play distinct physiological roles comes from naturally occurring mutations in mice and humans. The founding member of the lipin family, lipin-1, is the defective gene product in the fatty liver dystrophy (*fld*) mouse (2), which carries a null mutation of *Lpin1*. This mouse exhibits generalized lipodystrophy, peripheral neuropathy, insulin resistance, and increased susceptibility to atherosclerosis (11–13). Consistent with its tissue distribution, lipin-1 contributes the majority of PAP activity in adipose tissue and muscle (6, 7). Lipin-1 is also expressed in peripheral nerve, where it is required for normal Schwann cell function (14), and in liver, where it plays a role in response to fasting and in hepatic lipoprotein secretion (5, 8, 15, 16). Mutations in human *LPIN1* have recently been detected and cause recurrent acute myoglobinuria in childhood (17), indicating a critical role for lipin-1 in human muscle function. Based on phenotypes resulting from human and mouse mutations, lipin-1 has a unique function *in vivo*.

Less is known about the roles of lipin-2 or lipin-3 because mutant mouse models for these family members have not been characterized. However, rare human mutations in the *LPIN2* gene cause Majeed syndrome, an inflammatory disorder characterized by chronic recurrent multifocal osteomyelitis, congenital dyserythropoietic anemia, and cutaneous inflammation (18, 19). These symptoms indicate that lipin-2 plays a nonredundant function *in vivo*. Three distinct *LPIN2* mutations have been identified in unrelated Arabic families. In one family, deletion of two nucleotides in the lipin-2 coding region leads to a premature stop codon in the first third of the protein (20), likely resulting in nonsense-mediated mRNA decay and no functional protein product. A second mutation occurs in the donor splice site for exon 17 of the *LPIN2* gene, which leads to readthrough of intron sequences adding 65 irrelevant amino acid residues before reaching a stop codon (21). Although both of these mutations would prevent production of full-length lipin-2 protein, the third known mutation is a point mutation that leads to a single amino acid substitution, S734L (20). The affected serine residue resides in the C-LIP domain downstream of the PAP active site and transcriptional coactivator motifs. This serine residue is conserved in all three lipin family members and across most species, suggesting a conformational requirement that is required either for catalytic activity and/or a transcriptional coactivator function.

Here we characterize the effect of mutating the conserved serine on the PAP activity, membrane translocation properties, and coactivator functions of lipin-1 and lipin-2. Also because the Majeed syndrome affects blood, bone, and skin, this raises the question of whether lipin-2 has a direct role in the functions of these tissues. To investigate this, we perform a detailed expression analysis of lipin-2 by *in situ* hybridization of whole mice and qPCR of tissues relevant to Majeed syndrome.

EXPERIMENTAL PROCEDURES

Animal Studies—C57BL/6J mice were obtained from the Jackson Laboratory (Bar Harbor, ME). All mice were fed Purina 5001 mouse chow and were maintained on a 12:12-h light:dark cycle. Animal studies were performed under approval of the UCLA and University of Alberta, Edmonton, Institutional Animal Care and Use Committees.

Lipin Expression Constructs and Site-directed Mutagenesis—V5 epitope-tagged lipin-1 and lipin-2 expression plasmids were generated as described previously (6). Site-directed mutagenesis was performed using the QuickChange site-directed mutagenesis kit (Stratagene). Oligonucleotides used are as follows: lipin-1A^{S721L} (f, TACAAGTTTCTCTATTGTTTAGCACGTGCCATTGGGATGGCGGAC, and r, GTCCGCCATCCCAATGGCACGTGCTAAACAATAGAGAAACTTGTA); lipin-1A^{S721D} (f, TACAAGTTTCTCTATTGTGACGCACGTGCCATTGGGATGGCGGAC, and r, GTCCGCCATCCCAATGGCACGTGCGTCACAATAGAGAAACTTGTA); lipin-2^{S731L} (f, TGGCTACAAGTTTCTGTACTGTTTAGCACGTGCCATCGGCATGGC, and r, GCCATGCCGATGGCACGTGCTAAACAGTACAGAAACTTGTAGCCA); and lipin-2^{S731D} (f, TGGCTACAAGTTTCTGTACTGTGACGCACGTGCCATCGGCATGGC, and r, GCCATGCCGATGGCACGTGCGTCACAGTACAGAAACTTGTAGCCA).

Cell Culture and Transfection—HEK 293 and Hepa 1–6 cells (American Type Culture Collection, Manassas, VA) were propagated in Dulbecco's modified Eagle's medium supplemented with 10% fetal bovine serum and antibiotics and incubated at 37 °C in 5% CO_2. Cells were transfected with Effectene (Qiagen). Two days after transfection, the cells were lysed and assayed for PAP or luciferase reporter activity.

PAP Activity—PAP assays were performed as described previously (6). Briefly, HEK 293 cells were homogenized in 0.25 M sucrose containing 2 mM dithiothreitol (to stabilize PAP activity), protease inhibitor mixture (EDTA-free, Roche Diagnostics), phosphatase inhibitor cocktails I and II (Sigma), and 0.15% Tween 20. We assayed PAP activity in a final volume of 0.1 ml containing 100 mM Tris maleate buffer, pH 7.5, 5 mM Mg^{2+}, and 0.6 mM PA labeled with [^{3}H]palmitate (about 75 Ci/mol) dispersed in 0.4 mM PC and 1 mM EDTA (22, 23). The final concentration of Tween 20 in the assay was adjusted to 0.05%. Reactions were stopped after incubation at 37 °C with 2.2 ml of chloroform containing 0.08% olive oil as carrier for neutral lipids. Then 0.8 g of basic alumina was added to adsorb the PA and any [^{3}H]palmitate formed by phospholipase A-type activities (23). The tubes were centrifuged, and 1 ml of the chloroform, which contains the [^{3}H]diacylglycerol product, was dried and quantitated by scintillation counting. Protein concentrations (measured by the Bradford method) and the times of incubation (normally 30 min) were adjusted so that $<$10% of the PA was consumed during the incubation. Total PAP activities were calculated from measurements at three different protein con-

centrations to ensure the proportionality of the assay. The activities measured in parallel assays containing 8 mM *N*-ethylmaleimide allowed us to estimate the contribution of lipid phosphate phosphatase activity to the total activity. This former activity was negligible compared with that of the overexpressed PAP activity, and therefore no correction was necessary in these experiments.

PAP activity was normalized to lipin protein expression by quantitative Western blot analysis. Equivalent amounts of protein from each sample were electrophoresed in 3–8% SDS-polyacrylamide gradient gels (Invitrogen) and transferred to nitrocellulose membranes using a semi-dry electroblotter (Bio-Rad). Membranes were blocked with 5% nonfat milk powder in Tris-buffered saline and incubated overnight with mouse monoclonal anti-V5 antibody conjugated to horseradish peroxidase (Invitrogen). Protein bands were detected using ECL-Plus chemiluminescent reagent (Amersham Biosciences). Fluorescent signal was detected with the Typhoon Imaging System and quantified with ImageQuant software.

Transcriptional Coactivation Assay—Hepa 1–6 cells were transiently transfected with a PPRE-firefly luciferase reporter plasmid along with phRL-TK-renilla luciferase control vector (Promega), pCMX-PPARα, pCMX-PGC-1α, pCMX-RXR (kindly provided by Dr. Peter Tontonoz), and wild-type or mutant lipin expression plasmids. As a negative control to demonstrate specificity of the response, the PPRE-Luc reporter was replaced with a mutant version in which the PPRE sequences were deleted (ΔPPRE). Two days after transfection, cells were washed in 1× phosphate-buffered saline and lysed in Passive Lysis Buffer (Promega), and luciferase assays were performed using the Dual-Luciferase assay system (Promega). Firefly luciferase activity was normalized to *Renilla* luciferase activity to account for differences in transfection efficiency. In each experiment, samples were analyzed in quadruplicate.

In Vitro Translocation Assay for Lipins—Measurement of the capacity of wild-type and mutant lipin-2 proteins to translocate to endoplasmic reticulum membranes was based upon our previous work (24). Livers of male Sprague-Dawley rats were perfused with 60 ml of sterile ice-cold phosphate-buffered saline, pH 7.4, and homogenized in 0.25 M sucrose containing 2 mM dithiothreitol and 20 mM HEPES buffer, adjusted to pH 7.4 with KOH. The homogenates were centrifuged at 4 °C for 15,300 × *g* for 20 min, and the supernatant was then centrifuged for a further 400,000 × *g* for 40 min to pellet the microsomal fraction. This pellet was resuspended at 37 °C in homogenization buffer containing 6 mg/ml fatty acid-free bovine serum albumin and incubated for 20 min to remove fatty acids and dissociate bound lipin from the membranes. The microsomal membranes were then collected after re-centrifuging at 4 °C as above and resuspended in the same buffer. Recombinant lipins were expressed in HEK 293 cells, which were then homogenized in 0.25 M sucrose containing 2 mM dithiothreitol and 20 mM HEPES buffer, and adjusted to pH 7.4 with KOH and phosphatase inhibitor cocktails 1 and 2 from Sigma. The mitochondria-free supernatant was then isolated after centrifugation for 16,000 × *g* for 20 min to collect lipin-2 bound to endoplasmic reticulum membranes and in the cytosol.

For the translocation experiments, 350 μg of liver microsomal protein was incubated for 5 min at 37 °C in a final volume of 20 μl of homogenizing buffer containing 6 mg/ml bovine serum albumin and 0–750 μM K^+ oleate. The extract from the HEK 293 cells containing recombinant lipin (about 250 μg of total protein) was added, and the tubes were then incubated for 10 min at 37 °C to equilibrate the lipins between cytosol and membrane fractions (24). Following this, the samples were cooled on ice for 5 min. The soluble proteins were then collected after centrifugation at 400,000 × *g* for 40 min at 4 °C. The pellets (membranes) were resuspended in 45 μl of homogenization buffer. The cytosolic fractions were treated with 4 volumes of acetone at −20 °C. The precipitated protein was collected by centrifugation and resolubilized in 45 μl of homogenization buffer. Samples for Western blotting were prepared with 4× NuPAGE LDS SB from Invitrogen and then stored at −80 °C.

PCR-Restriction Fragment Length Polymorphism Assay—Total RNA was isolated from C57BL/6J mouse liver with TRIzol (Invitrogen), and cDNA was synthesized from 1 μg of RNA using Omniscript reverse transcriptase kit (Qiagen, Valencia, CA). The PCR-restriction fragment length polymorphism assay was performed by simultaneous amplification of lipin-2 and lipin-1 using the following primers (f, ACCATCTACC-TGTGGAA, and r, AGAAACTTGTAGCCATTCT), followed by restriction enzyme digestion of amplified fragment with either EcoRV or PvuII (New England Biolabs). Products were analyzed by electrophoresis in 2% agarose.

In Situ Hybridization—To generate templates for sense and antisense RNA generation, we PCR-amplified a 661-bp fragment of mouse lipin-2 cDNA (oligonucleotide primers f, cttcctaggccaccactcag, and r, tgaaataatctgccccaagg) and subcloned it into pCR 2.1-TOPO (Invitrogen). Plasmids were sequences to select templates for sense and antisense probe generation and linearized by digestion with BamHI. *In situ* hybridization was performed using the services of Phylogeny, Inc. (Columbus, OH). ^{35}S-UTP-labeled cRNA of transcripts was synthesized by *in vitro* transcription and hybridized to mouse whole body or tissue sections. Whole body sections were prepared from adult mice fasted for 4–5 h in the morning before sacrifice. Additional tissues were prepared from animals with and without fasting, as indicated. Sections were frozen, cut into 10 μM thick sections, mounted on gelatin-coated slides, and stored at −80 °C. Sections were then hybridized overnight at 55 °C in 50% deionized formamide, 0.3 M NaCl, 20 mM Tris-HCl, pH 7.4, 5 mM EDTA, 10 mM NaH_2PO_4, 10% dextran sulfate, 1× Denhardt's, 50 μg/ml total yeast RNA, and 50,000–80,000 cpm/μl ^{35}S-labeled cRNA probe. The tissues were subjected to stringent washing at 65 °C in 50% formamide, 2× SSC, 10 mM dithiothreitol and washed in phosphate-buffered saline before treatment with 20 μg/ml RNase A at 37 °C for 30 min. Following washes in 2× SSC and 0.1× SSC for 10 min at 37 °C, the slides were dehydrated, exposed to Kodak BioMaxMR x-ray film for 2–5 days, and then dipped in Kodak NTB nuclear track emulsion and exposed in light-tight boxes with desiccant at 4 °C for 10–15 days. Photographic development was carried out in Kodak D-19. Slides were counterstained lightly with hematoxylin and analyzed using both light and dark field optics. Sense control cRNA probes (identical to the mRNAs) always gave background levels of hybridization signal.

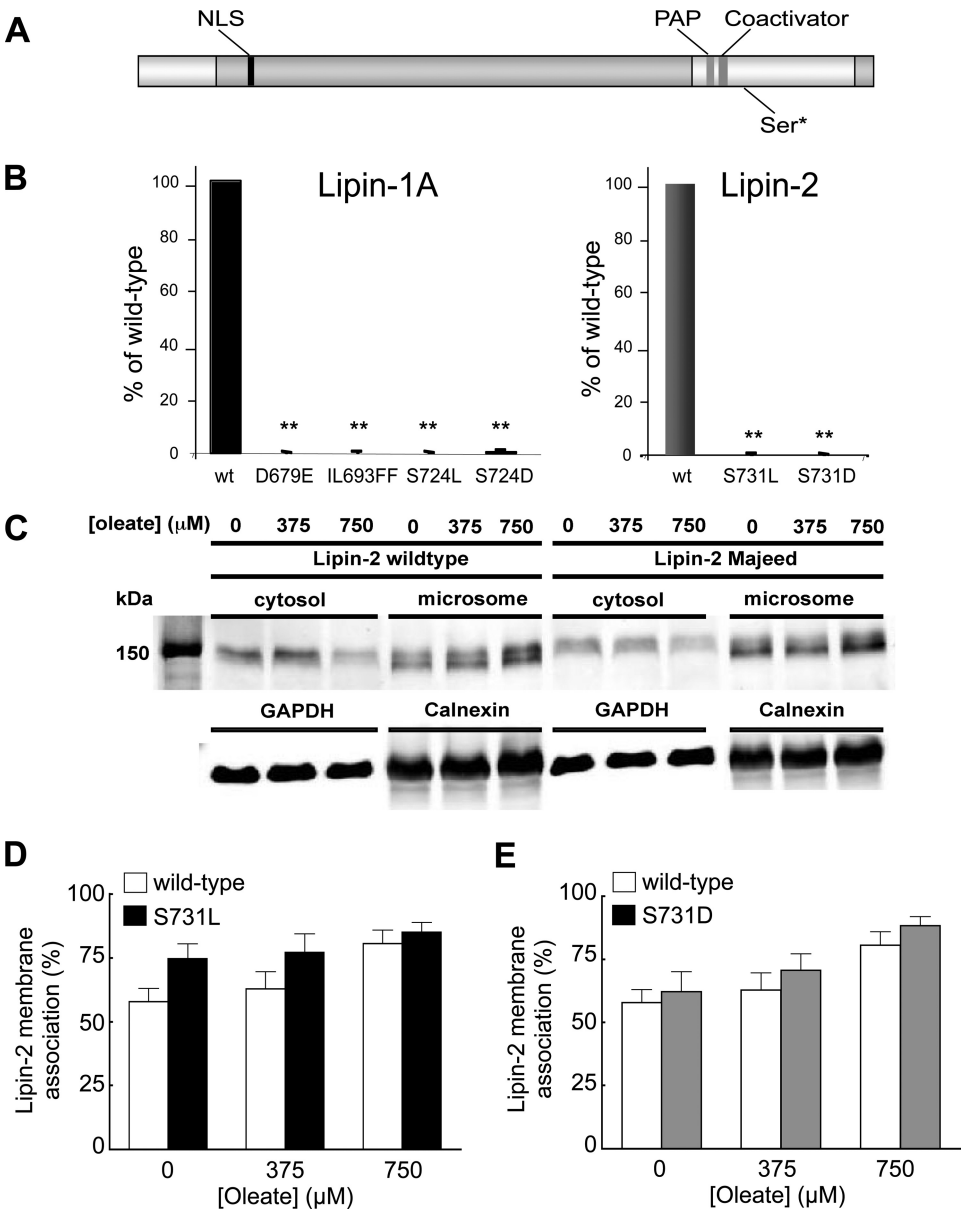

FIGURE 1. **Majeed serine to leucine substitution abolishes lipin-2 PAP activity but does not prevent membrane association.** *A,* lipin proteins contain evolutionarily conserved N-LIP (~125 amino acids) and C-LIP (~200 amino acids) domains as well as functional motifs that include a nuclear localization signal (*NLS*), a PAP Mg^{2+}-dependent phosphatase motif, and a transcriptional coactivator interaction motif. A point mutation that affects a conserved serine (*Ser**) within the C-LIP domain of human lipin-2 causes Majeed syndrome. *B,* Majeed syndrome serine to leucine mutation was generated in analogous residues of mouse lipin-1A (S724L) and lipin-2 (S731L). Mutation to an aspartate residue was also performed (S724D and S731D in lipin-1A and lipin-2, respectively). As controls that are known to abolish PAP activity, we also mutated the PAP motif (D679E) and coactivator motif (IL693FF) in lipin-1A. The indicated recombinant lipin proteins tagged with a V5 epitope were expressed in HEK 293 cells, and PAP activity was determined in cell lysates 2 days after transfection. The PAP activity in cells transfected with empty vector was less than 1% that for cells expressing lipin-1A and was subtracted from all other values. The relative specific activity of the lipins was then calculated by normalizing to the protein expression level, determined by Western blot analysis. The results are shown relative to the specific activity of lipin-1A or lipin-2 (*left* and *right panels*, respectively) and are given as mean ± S.D. **, $p < 0.0005$ *versus* wild-type (*wt*) lipin-1A or lipin-2. *C, in vitro* cytosol/membrane partitioning assay for wild-type and mutant lipin-2 proteins. Representative Western blot shows the translocation of lipin-2 isoforms from the cytosol to microsomal membranes when stimulated with increasing concentrations of oleate (0, 375, and 750 μM, as indicated *above lanes*). The *bottom panel* shows the cytosolic protein control (glyceraldehyde-3-phosphate dehydrogenase, *GAPDH*) and the microsomal protein control (*calnexin*) to which lipin-2 levels were normalized. *D,* quantitation of membrane bound wild-type and lipin-2^{S731L} from the cytosol/membrane partitioning assay. The lipin-2 bands from three experiments were quantified, and the means ± S.D. from three independent experiments are expressed as the percent of lipin-2 in the microsomal membranes at indicated oleate concentrations. *E,* quantitation of membrane bound wild-type and lipin-2^{S731D} from the cytosol/membrane partitioning assay.

qPCR of Lipin Gene Expression in Mouse Tissues—Blood and tissues were isolated from adult male C57BL/6J mice. Red blood cells were isolated from fresh whole blood after centrifugation at 200 × *g* for 10 min at 4 °C. The spleen was divided into two pieces, and the white blood cell fraction was isolated from one piece by selective lysis of erythrocytes using 2.5 ml of lysis buffer (0.15 M NH_4Cl, 10 mM $KHCO_3$, 0.1 mM Na_2EDTA), incubating at room temperature for 5 min, and collecting remaining cells (enriched in lymphocytes) by centrifugation at 200 × *g* for 10 min. Cells were washed in phosphate-buffered saline containing 3% fetal bovine serum, and the final pellet was used for RNA isolation. RNA and cDNA were prepared from blood cells or flash-frozen tissues (liver, spleen, and thymus) as described above. qPCR was performed with SYBR Green as described previously (6, 25). Primers were as follows: lipin-1, GCTCCCGAGAGAAAG-TGGTGGA, GGCTTTCCATTCT-CGCAGCTCCT; lipin-2, AGTTG-ACCCCATCACCGTAG, CCC-AAAGCATCAGACTTGGT; and lipin-3, TGGAATTGGGATGA-CAAGGT, CACTGCAAGTACC-CCTTGGT.

Statistical Analysis—Experimental groups were compared with appropriate control groups as indicated in the figure legends using the Student's *t* test and were considered statistically significant for $p < 0.05$.

RESULTS

Mutating the Majeed Serine Residue Abolishes PAP Enzyme Activity—The Majeed S734L mutation in human lipin-2 alters a serine residue that is located in the C-LIP domain downstream of the enzyme active site and coactivator motifs (Fig. 1*A*). The affected serine residue is conserved in lipin-1, -2, and -3 in mammals and in orthologous proteins in other species. We investigated the biochemical basis for the Majeed syndrome in individuals carrying an S734L missense mutation in lipin-2 by analyzing PAP

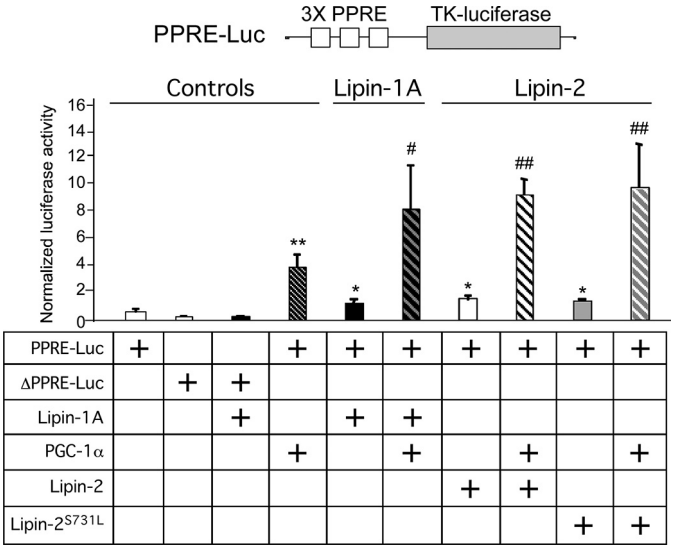

FIGURE 2. **Wild-type and Majeed lipin-2 proteins exhibit transcriptional coactivator activity with PGC-1α on the PPRE.** The effect of lipin-2 on transcriptional activity of a luciferase reporter containing the multimerized 3× PPRE upstream of a viral thymidine kinase minimal promoter. Hepa 1–6 cells were cotransfected with a luciferase reporter (PPRE-Luc, containing the multimerized 3× PPRE upstream of a viral thymidine kinase minimal promoter) and PPARα and retinoid X receptor expression vectors; transfections also contained PGC-1α and/or lipin expression vectors, as indicated. A mutated PPRE (ΔPPRE), which is unresponsive to PGC-1α, served as a control to demonstrate specificity. Firefly luciferase activity from PPRE-Luc was normalized to *Renilla* luciferase from a control plasmid that was included in each transfection. *Bars* represent the mean relative luciferase activity ± S.D. of four replicate transfections for each group. *, $p < 0.05$ *versus* PPRE-Luc; **, $p < 0.01$ *versus* PPRE-Luc; #, $p < 0.05$ *versus* PGC-1α; ##, $p < 0.01$ *versus* PGC-1α.

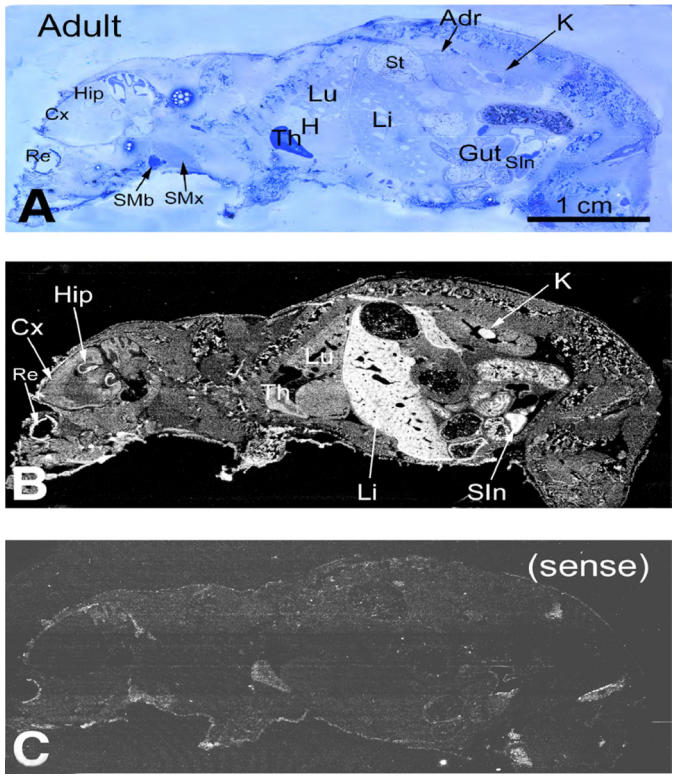

FIGURE 3. ***In situ* hybridization detects prominent lipin-2 expression in liver, kidney, brain, and thymus of adult mouse.** *A,* anatomical view under bright field illumination of an adult mouse whole body section after *in situ* hybridization with an antisense probe for lipin-2 and counter-staining with hematoxylin. *B,* x-ray film autoradiography of section adjacent to that shown in *A*, following hybridization with a lipin-2 antisense riboprobe. *C,* x-ray film autoradiography of section adjacent to that shown in *A*, following hybridization with a control lipin-2 sense riboprobe. Abbreviations used are as follows: *Adr,* adrenal; *Cx*, brain cortex; *Hip*, hippocampus; *K*, kidney; *Li*, liver; *SIn*, small intestine; *St*, stomach; *SMb*, submandibular gland; *SMx*, submaxillary gland; *Th*, thymus; *Re*, retina; *H*, heart; *Lu*, lung.

activity of recombinant mouse lipin-2 with a leucine substitution at the analogous serine residue, Ser 731. We also produced the corresponding mutation in mouse lipin-1A at Ser 724. Lipin-1 protein occurs in two forms (lipin-1A and lipin-1B) that result from alternative mRNA splicing, both of which have PAP activity (6). The lipin-1A splice variant was utilized in all studies described here. We expressed lipin-1A^{S724L} and lipin-2^{S731L} in HEK 293 cells and determined PAP activity in cell lysates. Wild-type lipin-1A and lipin-2 served as positive controls.

Wild-type lipin-1A and lipin-2 had robust PAP activity (63 ± 8.4 and 36 ± 3.1 nmol/mg/min, respectively) (Fig. 1*B*). As expected, mutation of the PAP motif (D679E) or the coactivator motif (IL693FF) abolished PAP activity, as has been reported previously (5). The serine to leucine substitution found in Majeed patients likewise completely abolished PAP activity in both lipin-1 and lipin-2 backgrounds. Wild-type lipin-2 and lipin-2^{S731L} proteins were expressed at similar levels, confirming that the lack of PAP activity is not related to reduced protein levels or protein stability (Fig. 1*C* and data not shown). Mutation of the Ser residue to aspartic acid likewise abolished PAP activity in both lipin-1A and lipin-2, indicating that activity cannot be restored by the presence of a negative charge (Fig. 1*B*).

PAP Deficiency of Lipin-2^{S731L} and Lipin-2^{S731D} Does Not Result from Impaired Membrane Association—Studies performed several years ago, prior to the molecular identification of the lipin proteins, demonstrated that PAP enzymes reside in the cytosolic compartment of the cell. They translocate reversibly to endoplasmic reticulum membranes to catalyze the PAP reaction when cells are stimulated with unsaturated rather than saturated fatty acids (24, 26). Although lipin-2 is known to associate largely with the endoplasmic reticulum when expressed in HeLa cells (10), fatty acid-induced translocation has never been directly demonstrated for lipin-2. Therefore, we investigated whether wild-type lipin-2 exhibits oleate-induced membrane translocation and whether membrane association is impaired by mutation of the Majeed serine residue. Combined membrane and cytosolic fractions from HEK 293 cells expressing similar levels of recombinant wild-type lipin-2 or lipin-2^{S731L} were used for these experiments rather than cytosolic fractions alone so as not to exclude forms of lipin-2 that might preferentially bind to membranes. These forms of lipin-2 were added to rat liver microsomes, which had been depleted of bound lipins by washing with albumin, in the presence of increasing oleate concentrations (0, 375, and 750 μM). This incubation allowed lipin-2 to redistribute between membrane and cytosolic fractions. The relative amounts of lipin-2 in the cytosol and membrane fractions that were re-isolated were determined by Western blot analysis. Cytosolic- and membrane-associated lipin-2 levels were normalized to levels of glyceraldehyde-3-phosphate dehydrogenase and calnexin, respectively, which do not alter their localization in the presence of oleate.

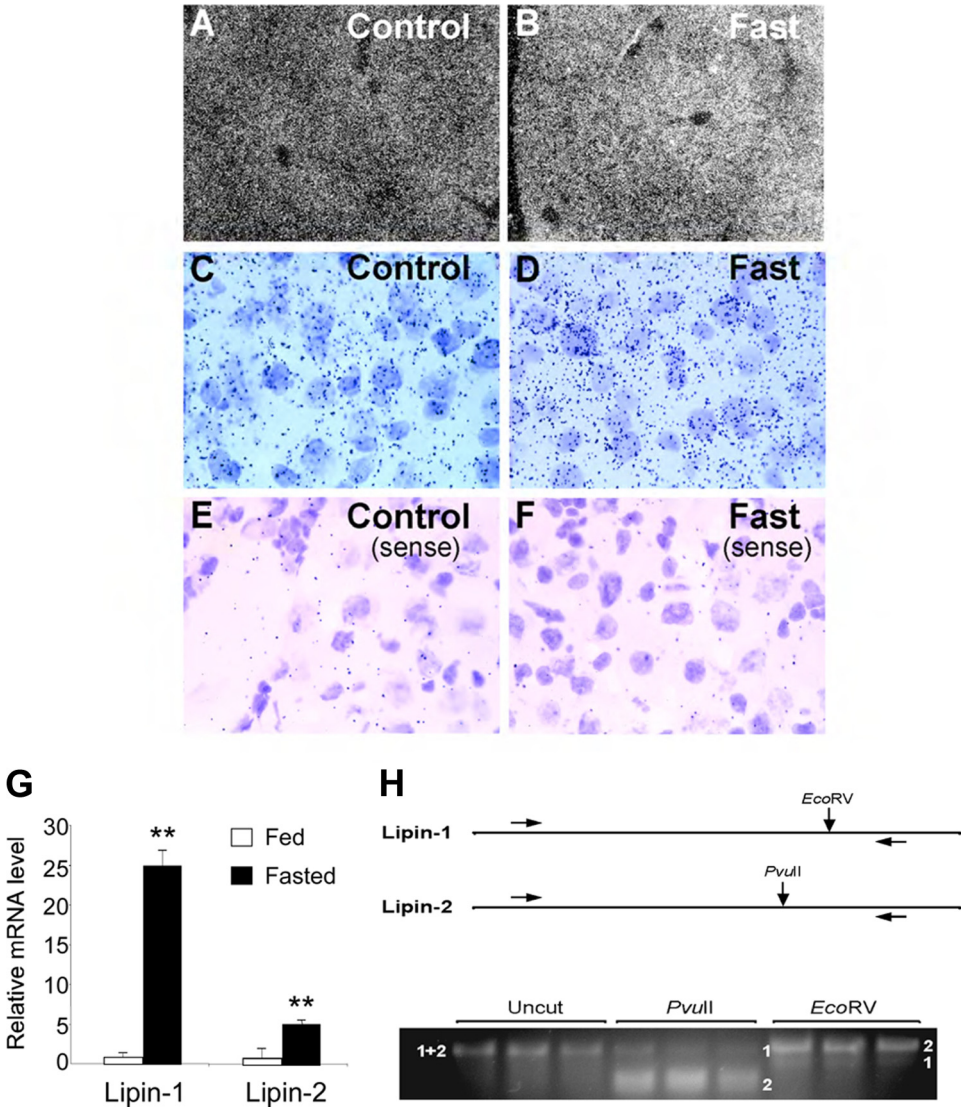

FIGURE 4. **Lipin-2 mRNA expression in hepatocytes is induced by fasting, and lipin-2 is expressed at higher levels in liver than lipin-1.** Visualization under dark field illumination of lipin-2 mRNA after *in situ* hybridization with an antisense probe in adult mouse liver sections under fed (*A*) or 14-h fasting conditions (*B*). Bright field illumination of hepatic lipin-2 antisense *in situ* hybridization of liver from control fed (*C*) and fasting conditions (*D*) shows signal occurring within hepatocytes; hepatocyte nuclei appear *dark blue*. Hybridization with a control sense probe shows minimal signal in fed (*E*) or fasted (*F*) adult mouse liver. *G*, real time RT-PCR quantitation of lipin-1 and lipin-2 mRNA shows 25- and 5-fold induction upon fasting, respectively. **, $p < 0.005$ *versus* fed mice. *H*, restriction fragment-length/PCR assay detects higher absolute level of lipin-2 than lipin-1 mRNA in liver. A 170-bp fragment of lipin-1 and lipin-2 cDNA from liver was simultaneously amplified by PCR using a single oligonucleotide primer set. The products derived from lipin-1 *versus* lipin-2 templates were distinguished by restriction enzyme digestion. EcoRV digestion of the lipin-1 product generates 125- and 45-bp fragments. PvuII digestion of the lipin-2 product generates 97- and 73-bp fragments. Products from liver samples of 3 fasted C57BL/6J mice are shown in *lower panel*. Amplification products were analyzed by agarose gel electrophoresis before and after restriction digestion with the indicated enzymes. Lipin-2 contributes the majority of the signal, indicating higher expression levels in liver than lipin-1.

Wild-type lipin-2 was present at similar levels in cytosolic and membrane fractions in the absence of oleate, and it translocated to the membrane fraction with increasing levels of oleate (Fig. 1, *C*, *left panel*, and *D*). Lipin-2^{S731L} showed no reduction in membrane association and in multiple trials exhibited a trend toward increased membrane localization compared with wild-type lipin-2, particularly in the absence of oleate (Fig. 1, *C*, *right panels*, *D*). However, there was no statistically significant difference in membrane localization between wild-type and mutant lipin-2 ($p = 0.09$, Student's *t* test). Likewise, the lipin-2^{S731D} protein exhibited normal membrane localization (Fig. 1*E*), suggesting that the amino acid residue at this position is not a determinant of membrane association. Significantly, wild-type as well as the S731L and S731D mutant forms of lipin-2 resolved into two bands (see Fig. 1*C*). The cytosolic lipin-2 consisted primarily of the slower migrating band, whereas the membrane-bound forms had a high proportion of the faster migrating band. This result is compatible with that for lipin-1 where a faster migrating species (hypophosphorylated lipin-1) associated preferentially with membranes (7, 10).

Thus, the defective action of lipin-2 in the Majeed syndrome cannot be attributed to a failure of the protein to associate with endoplasmic reticulum membranes. It remains possible, however, that the mutant lipin-2 protein assumes an abnormal configuration in its membrane interaction that could affect catalysis.

Lipin-2 Amplifies PGC-1α-mediated Transcriptional Coactivation, and the Majeed Mutation Does Not Impair Coactivator Activity—Lipin-1 functions as a coactivator in the PGC-1α/PPARα pathway, leading to transcriptional coactivation of PPARα target genes in hepatocytes (5). Because the PPAR-binding motif present in the C-LIP domain of lipin-1 is conserved in lipin-2, we tested the ability of lipin-2 to coactivate transcription through a PPRE. Transcriptional coactivation assays were performed using a PPRE-luciferase (PPRE-Luc) reporter gene in Hepa 1–6 hepatoma cells. Cells were transfected with the reporter construct and PPARγ and retinoid X receptor-α expression vectors in the presence and absence of PGC-1α and wild-type or mutant lipin expression constructs. Similar to previous results for lipin-1B (5), lipin-1A activated PPRE-luciferase expression ~2-fold (Fig. 2, compare *bars* for lipin-1A to PPRE-Luc) and amplified the effect of the PGC-1α coactivator (compare activity of PGC-1α + lipin-1A with that of PGC-1α alone). This effect required a functional PPRE, as deletion of this regulatory element (ΔPPRE-Luc) prevented activation. Lipin-2 had nearly identical coactivator activity as lipin-1, showing modest activation of the reporter on its own (compare lipin-2

with PPRE-luc) and amplifying of the effect of PGC-1α (compare PGC-1 α + lipin-2 with PGC-1 α). Notably, the lipin-2^{S731L} mutant showed identical coactivator activity to wild-type lipin-1A and lipin-2. Thus, the serine that is required for PAP activity of both lipin-1 and lipin-2 is not required for coactivator function.

Lipin-2 Gene Expression in Liver, Digestive Tract, Red Blood Cells, and Lymphoid Cells—We previously demonstrated using qPCR that the three lipin genes have distinct, but overlapping, expression patterns across a panel of several mouse and human tissues (6). To obtain a more complete view of lipin-2 tissue expression throughout the body, including tissues that are affected in Majeed syndrome such as bone and skin, we used *in situ* hybridization with antisense lipin-2 RNA on whole mouse sections. Hybridization was observed at extremely high levels in the liver, as well as in specific regions of the gastrointestinal tract, kidney, and brain (Fig. 3). As a negative control, hybridization was performed with lipin-2 sense strand probe and showed minimal background hybridization, primarily in skin and retina (Fig. 3*C*).

In the liver, lipin-2 showed a uniform distribution pattern (Fig. 4) with labeling observed within hepatocytes (hepatocyte nuclei are visible as darkly stained areas in Fig. 4, *C–F*). Fasting for 14 h increased labeling by 2-fold (compare Fig. 5, *C* and *D*). It has been shown that lipin-1 is expressed in liver, where it is also induced by fasting (5). Using qPCR, we determined that fasting induces hepatic lipin-1 by 25-fold and lipin-2 by 5-fold (Fig. 4*G*). Thus far, it has been unclear whether lipin-1 or lipin-2 is expressed at higher absolute levels in the liver. To address this, we designed an assay to PCR-amplify lipin-1 and lipin-2 cDNA simultaneously with the same primer set and then to distinguish the products by restriction enzyme digestion (Fig. 4*H*). The PCR primers amplified a 170-bp fragment from both lipin-1 and lipin-2 cDNA. Subsequent digestion of the amplified product with PvuII cut the lipin-2 fragment into 97- and 73-bp fragments but did not alter lipin-1. In contrast, digestion with EcoRV cut the lipin-1 fragment to produce 125- and 45-bp fragments but did not cut lipin-2 (Fig. 4*H*). Both restriction reactions showed that lipin-2 mRNA levels in liver are substantially higher than lipin-1 levels, suggesting that lipin-2 may significantly contribute to PAP activity and lipin-associated coactivator activity in this tissue.

In addition to liver, *in situ* hybridization revealed significant levels of lipin-2 expression in the gastrointestinal tract. Expression was detected in squamous keratinized epithelium of the tongue and the esophagus, the epithelial cell layer of the intestinal mucosa, and in epithelial cell villi of the duodenum, ileum, and jejunum (Fig. 5). Lipin-2 expression in kidney was detected in the cortex, medulla, and papillae (results not shown). In brain, lipin-2 was expressed in the cortex, hippocampus, thalamus, and hypothalamus (Fig. 3*B* and results not shown). Lipin-2 was also expressed in the submandibular and submaxillary salivary glands, as well as the thymus and lung (Fig. 3*B*). Notably, we did not detect lipin-2 expression using *in situ* hybridization in bone or skin, tissues that show pathologic changes in Majeed syndrome (18, 19). The lack of lipin-2 expression in skin was confirmed using the extremely sensitive method of real time PCR; in contrast, lipin-1 mRNA could be detected at low levels

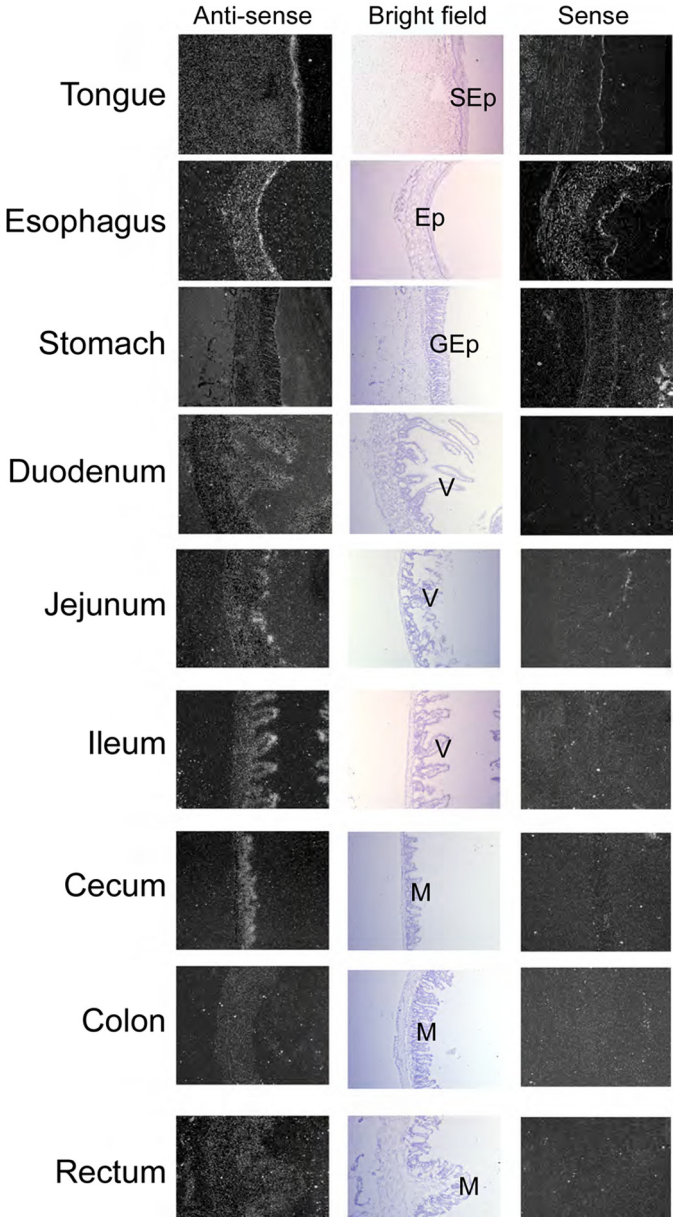

FIGURE 5. **Lipin-2 expression in the epithelial cell layer in tissues of the alimentary and digestive tract.** *In situ* hybridization was performed on adult mouse tissues using antisense probes to detect lipin-2 mRNA (*left panels*) or sense probes as a negative control (*right panels*). Corresponding bright field images of hematoxylin-stained sections are shown in the *middle panels*. Lipin-2 mRNA was detected in the tongue within the squamous keratinized epithelium (*SEp*), in esophagus within the epithelial cell layer (*Ep*), and within villi epithelial cells (*V*) of the duodenum, jejunum, ileum, and in mucous (*M*) of the cecum. Lipin-2 mRNA was not detected in the glandular epithelium (*GEp*) of the stomach, colon, nor rectal mucosa (*M*).

in skin (Fig. 6*A*). We detected low levels of lipin-2 expression in bone and bone marrow, at 10–20% the levels in liver (Fig. 6*A*).

We also assessed whether the anemia and inflammatory conditions observed in Majeed syndrome may reflect a role for lipin-2 in red blood cells and lymphoid cells. Using qPCR, we detected mouse lipin-2 expression in circulating red blood cells, in whole spleen and the white blood cell fraction of spleen, and in thymus, all at ~10% of the levels observed in liver, where lipin-2 is expressed at highest levels (Fig. 6*B*). Although direct comparisons of gene expression among all three lipin genes are

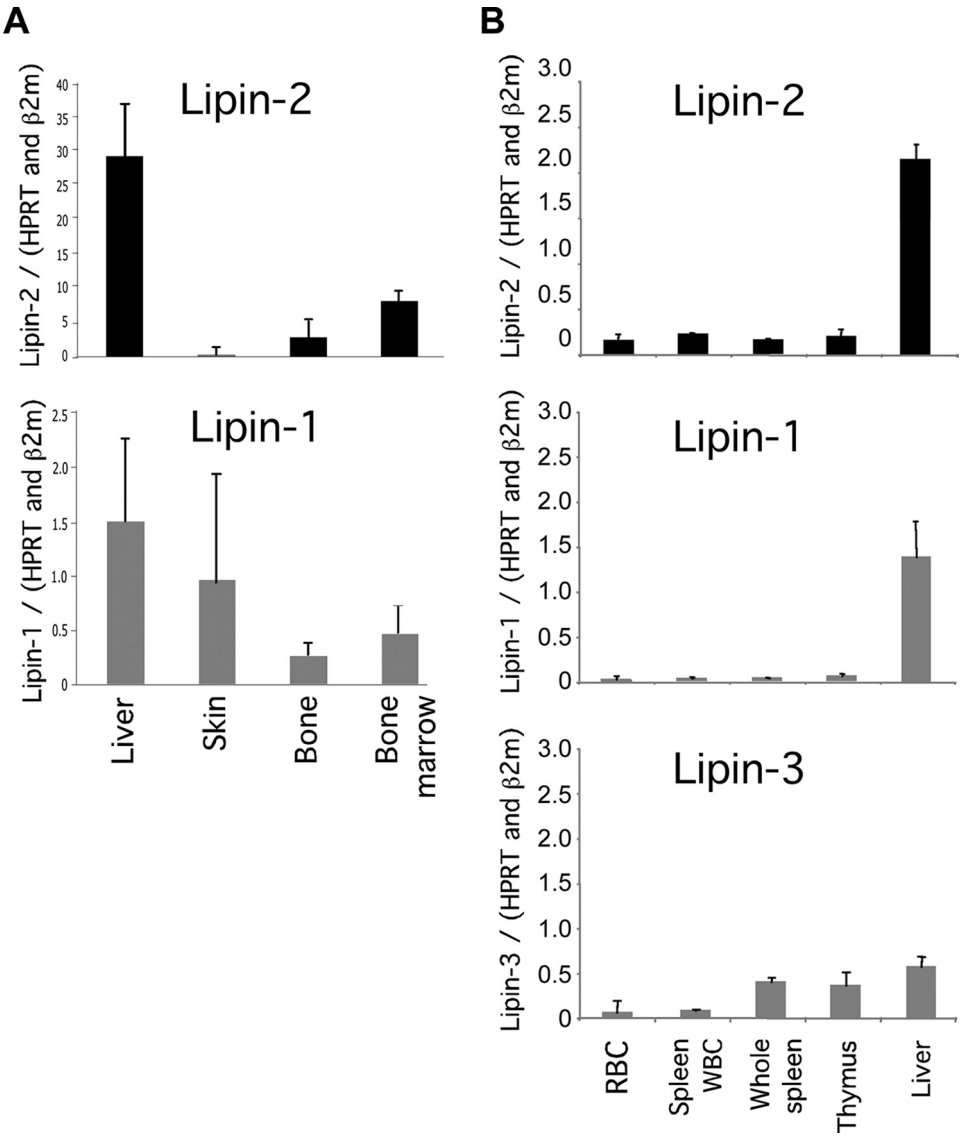

FIGURE 6. **Analysis of lipin gene expression in skin, bone, bone marrow, erythrocytes, and lymphoid tissues.** Relative lipin gene expression levels were determined by qPCR in skin, bone, and bone marrow (*A*), and in red blood cells (*RBC*), whole spleen, the white blood cell fraction of spleen (*WBC*), and thymus (*B*) of adult C57BL/6J mice ($n = 5$; values represent mean ± S.D.). Samples prepared from bone were first flushed to remove bone marrow. Lipin-1, lipin-2, and lipin-3 mRNA levels were normalized to expression of β_2-microglobulin (*β2m*) and hypoxanthine phosphoribosyltransferase (*HPRT*). The expression levels of each lipin mRNA in liver are shown to demonstrate that absolute values in most tissues are likely much higher for lipin-2, because liver expression levels are much higher for lipin-2 than lipin-1 and lipin-3.

not possible using different PCR primer sets, based on the determination that lipin-2 is expressed at much higher levels in liver than lipin-1 or lipin-3 (Fig. 4*H*) (6), lipin-2 appears to be the prominent lipin mRNA expressed in red blood cells and lymphoid tissues (Fig. 6).

DISCUSSION

Our first objective was to determine the functional significance of the serine that is mutated in the Majeed syndrome and that is conserved in lipin proteins from different species. The S734L mutation occurs within the C-LIP domain that is evolutionarily conserved among lipin family members but is distinct from the previously defined catalytic and transcriptional coactivator protein motifs. Mutation of the serine to leucine or aspartate abolishes the PAP activity of lipin-1 and lipin-2. Nevertheless, the mutant lipin-2 protein was able to associate with membranes, a key step in the physiological expression of PAP activity. We also provide the first evidence that wild-type lipin-2 exhibits transcriptional coactivator activity equivalent to lipin-1. This coactivator function is retained when the Majeed serine residue is mutated. Our results define the conserved serine as critical for the function of lipins as enzymes, and suggest that a primary defect in Majeed syndrome is the loss of lipin-2 PAP activity.

It is notable that orthologous lipin protein sequences in all multicellular organisms, including invertebrates and plants, have serine at the position affected by the Majeed mutation, whereas most single-celled organisms have a threonine residue (Fig. 7*A*). This suggests that the presence of a hydroxyl group at this position is critical for the conformation of the lipins with respect to their phosphatase activity. This conclusion is compatible with the crystallographic structures of the haloacid dehalogenase (HAD)-like superfamily of proteins (27) to which the lipins belong. The HAD-like proteins possess four conserved motifs (I–IV) that are essential for HAD domain catalytic activity as follows: I, a β-strand followed immediately by the D*X*D*X*T catalytic motif; II, a β-strand followed immediately by a conserved Ser/Thr residue, which is involved in coordinating the phosphate group to be hydrolyzed in the catalytic site of the HAD-type proteins (27); and III and IV, two α-helices flanking motif II. The secondary structures surrounding the active sites of lipin-1 and lipin-2 are predicted to possess the same structural organization as previously characterized HAD protein family members (Fig. 7*B*). The serine residue in the predicted HAD motif II is essential because we showed that lipin-1A^{S721L}, lipin-1A^{S721D}, lipin-2^{S731L}, and lipin-2^{S731D} were devoid of PAP activity. Therefore, we conclude that the hydroxyl group of serine or threonine in this position is also essential for the correct conformation of the active site of lipin family members. Final proof for this awaits the availability of a lipin protein crystal structure.

Importantly, the studies reported here also establish that lipin-2 can function as a transcriptional coactivator for PGC-

A

Vertebrates	h Lipin-2	709	Y H S I N E N G Y K F L T C S A R A I G M A D M T R G Y L	737
	m Lipin-2	743	Y H S I N E N G Y K F L Y C S A R A I G M A D M T R G Y L	771
	h Lipin-1	720	Y H K V S Q N G Y K F L Y C S A R A I G M A D M T R G Y L	748
	m Lipin-1	717	Y H K V S Q N G Y K F L Y C S A R A I G M A D M T R G Y L	745
	h Lipin-3	675	Y H K I Q L N G Y K F L Y C S A R A I G M A D L T R G Y L	703
	m Lipin-3	672	Y H K I H L N G Y K F L Y C S A R A I G M A D L T R G Y L	700
	Gallus gallus	675	Y H S I N E N G Y K F L Y C S A R A I G M A D M T R G Y L	703
	Xenopus laevis	706	Y H T I H E N G Y K F L Y C S A R A I G M A D M T R G Y L	734
	Danio rerio Chr 20	422	Y H N V S Q N G Y K F L Y C S A R A I G M A D M T R G Y L	450
	Danio rerio Chr 17	716	Y H R V S Q N G Y K F M Y C S A R A I G M A D M T R G Y L	744
Invertebrates	*Drosophila melanogaster*	843	F S K I E Q N G Y K L L Y L S A R A I G Q S R V T R E Y L	871
	Anopheles gambiae	923	F S K I E E N G Y K M L Y L S A R A I G Q A K T T R G Y L	951
	Caenorhabditis elegans	590	Y T R I K N N G Y K M V Y L S S R A I G Q S H T T K Q Y L	618
Single-celled	*Saccharomyces cerevisiae*	429	F S E I S R N G Y N I L Y L T A R S A G Q A D S T R S Y L	457
	Schizosaccharomyces pombe	414	Y T D I T N N G Y K I M Y L T S R S V G Q A D S T R H Y L	442
	Plasmodium falciparum	991	F N K I N K N G Y H I L Y L T A R A I G Q A D S T R E Y L	1019
	Leishmania major strain Friedlin	718	Y S K I E F N G Y R M V Y L T A R S V S Q I N Q T K S Y L	746
	Tetrahymena thermophila	706	Y Q N I V K N G Y Q I L Y L T A R A I G Q S E Q T R K F I	734
	Cryptosporidium muris	442	L T K I E E N G Y K I I Y L T A R A I G Q A D A T R D F L	470
Plants	*Arabidopsis thaliana* Chr 3	738	F S A I K E N G Y Q L L F L S A R A I V Q A Y L T R N F L	766
	Arabidopsis thaliana Chr 5	765	F S A V K E N G Y Q L I F L S A R A I S Q A S V T R Q F L	793
	Oryza sativa Chr 1	387	P Y V V M E N G Y Q L L F L S A - - I I Q A Y L T K N F L	413
	Oryza sativa Chr 11	1220	F S A I K E N G Y Q L L F L S A R A I S Q A H L T R Q F L	1248

B

Lipin-1A 674 KVIISDIDGTITRSDTLGHILPTLGKDWTHQGIAKLYHKVSQNGYKFLYCSARAIGMAD
Lipin-2 681 KVIISDIDGTITKSDALGQILPQLGKDWTHQGIARLYHSINENGYKFLYCSARAIGMAD

Predicted HAD motif I
Predicted HAD motif II

Lipin-1A 733 MTRGYLHWVNERGTVLPQGPLLLSPSSLFSALHREVIEKKPEKFKVQCLTDIKNL----
Lipin-2 740 MTRGYLHWVNDKGTILPRGPLMLSPSSLFSAFHREVIEKKPEKFKIECLNDIKNL----

Predicted HAD motif II
Predicted HAD motif III

Lipin-1A 795 FYAAFGNRP-DVYSYKQVGVSLNRIFTVNPKGE
Lipin-2 802 FYAAFGNRP-DVYAYTQVGVPDCRIFTVNPKGE

Predicted HAD motif IV

FIGURE 7. **Majeed serine residue conservation and position within catalytic domains.** *A,* multispecies alignment of amino acid sequence surrounding the serine residue mutated in Majeed syndrome. Residues that are conserved among all vertebrate lipin proteins are shaded in *yellow*; the position of the serine residue affected in Majeed syndrome is *boxed*. As shown, the serine is conserved in vertebrate, invertebrate, and plant species. In single-celled eukaryotes, however, the corresponding residue is a threonine. *h*, human; *m*, mouse. *B,* secondary structure surrounding the catalytic motif for mouse lipin-1 and lipin-2 was predicted by jnet algorithms using the jpred server. Similar structures were predicted by using the jhmm and jpssm algorithms (results not shown). *Green arrows* indicate predicted β-strands, and *blue boxes* indicate predicted α-helices. Conserved amino acids from the HAD family of proteins are shown in *red letters*. The predicted HAD motifs around the active site of the lipins are conserved in all of the HAD-like proteins that have been studied by x-ray crystallography (27).

1α/PPARα, as demonstrated previously for lipin-1 (5). The serine to leucine substitution occurring in Majeed syndrome did not compromise lipin-2 coactivator function, indicating that the proposed requirement of this serine for the conformation of the catalytic site does not affect the presentation of the L*XX*IL motif. Also, we conclude that symptoms observed in patients

with the S734L Majeed mutation cannot be attributed to a lack of lipin-2 coactivator activity. By contrast, Majeed patients with nonsense mutations would experience a loss of both lipin-2 PAP and coactivator function. It is interesting to note that these patients have somewhat more severe symptoms than patients with the serine missense mutation. Whereas all patients experience osteomyelitis with joint pain, fever, and dyserythropoietic anemia, those with the nonsense mutation experienced more severe fever and anemia and required frequent blood transfusions (20). It is therefore possible that loss of both lipin-2 PAP and coactivator activities is more detrimental than the exclusive loss of PAP activity; however, because of the small number of patients available, it is not possible to exclude background genetic or environmental factors as determinants of these phenotypic differences.

It has not been possible to determine the mechanisms by which lipin-2 mutation results in the symptoms observed in Majeed syndrome because of the very small number of human patients and the limitations of such studies in humans. Instead, we performed a thorough characterization of tissues and cell types in which lipin-2 is expressed in the mouse to provide clues about its function in normal physiology and the consequences of its loss of function in Majeed syndrome. In agreement with our previous quantitative PCR results on a panel of eight tissues (6), the liver showed the highest lipin-2 expression. Using a PCR-restriction fragment length polymorphism assay, we determined that hepatic lipin-2 mRNA levels are substantially higher than those of lipin-1 mRNA, consistent with an important role for lipin-2 PAP activity in the liver (9). Furthermore, we visualized lipin-2 expression within the hepatocytes, revealing that it is not limited to secondary hepatic cell populations, such as Kupffer, Ito, or stellate cells. The *in situ* hybridization studies also revealed regional localization of lipin-2 in brain (hippocampus, cortex, and other areas), kidney (cortex, medulla, and papillae), and areas of the gastrointestinal tract (epithelial cell layers in regions extending from tongue to the small intestine).

We also detected lipin-2 expression in circulating red blood cells and lymphoid tissues, including spleen, thymus, and bone marrow. Lipin-2 PAP deficiency in these tissues could potentially contribute to the anemia and inflammation associated with Majeed syndrome. The mechanism(s) by which lipin-2 PAP deficiency could be pathogenic are unknown, but likely possibilities are suggested by studies of lipin-1 deficiency in mice and humans. Loss of lipin-2 PAP activity may be detrimental to cells that rely on this protein for synthesis of phosphatidylcholine, phosphatidylethanolamine, and triacylglycerol, the key downstream products that depend on diacylglycerol formed by PAP. Such effects are observed, for example, in lipin-1-deficient mice, which are lipodystrophic and insulin-resistant because of an inability to synthesize and store triacylglycerols in adipose tissue (13, 28). Another potential detrimental effect of lipin-2 PAP enzyme deficiency is the accumulation of lipid intermediates, such as PA, which acts as a signaling molecule within the cell (29–32). Indeed, deletion of *Lpin1* in Schwann cells leads to PA accumulation. This activates the mitogen-activated protein kinase kinase/extracellular-regulated kinase signaling pathways leading to demyelination, which contributes to the peripheral neuropathy in mice (14). PA accumulation in skeletal muscle as a result of mutation of the *LPIN1* gene in human beings is associated with myopathy (17).

Future studies in a lipin-2-deficient mouse model should shed further light on the physiological role of lipin-2 in glycerolipid synthesis, cell signaling by PA and DAG, and in the cotranscriptional regulation that we describe in this study. This work should also elucidate the consequences of lipin-2 deficiency in the pathology of Majeed syndrome.

Acknowledgment—We thank Ping Xu for excellent technical assistance.

REFERENCES

1. Reue, K., and Brindley, D. N. (2008) *J. Lipid Res.* **49,** 2493–2503
2. Péterfy, M., Phan, J., Xu, P., and Reue, K. (2001) *Nat. Genet.* **27,** 121–124
3. Han, G. S., Wu, W. I., and Carman, G. M. (2006) *J. Biol. Chem.* **281,** 9210–9218
4. Carman, G. M., and Han, G. S. (2009) *J. Biol. Chem.* **284,** 2593–2597
5. Finck, B. N., Gropler, M. C., Chen, Z., Leone, T. C., Croce, M. A., Harris, T. E., Lawrence, J. C., Jr., and Kelly, D. P. (2006) *Cell Metab.* **4,** 199–210
6. Donkor, J., Sariahmetoglu, M., Dewald, J., Brindley, D. N., and Reue, K. (2007) *J. Biol. Chem.* **282,** 3450–3457
7. Harris, T. E., Huffman, T. A., Chi, A., Shabanowitz, J., Hunt, D. F., Kumar, A., and Lawrence, J. C., Jr. (2007) *J. Biol. Chem.* **282,** 277–286
8. Manmontri, B., Sariahmetoglu, M., Donkor, J., Bou Khalil, M., Sundaram, M., Yao, Z., Reue, K., Lehner, R., and Brindley, D. N. (2008) *J. Lipid Res.* **49,** 1056–1067
9. Gropler, M. C., Harris, T. E., Hall, A. M., Wolins, N. E., Gross, R. W., Han, X., Chen, Z., and Finck, B. N. (2009) *J. Biol. Chem.* **284,** 6763–6772
10. Grimsey, N., Han, G. S., O'Hara, L., Rochford, J. J., Carman, G. M., and Siniossoglou, S. (2008) *J. Biol. Chem.* **283,** 29166–29174
11. Langner, C. A., Birkenmeier, E. H., Ben-Zeev, O., Schotz, M. C., Sweet, H. O., Davisson, M. T., and Gordon, J. I. (1989) *J. Biol. Chem.* **264,** 7994–8003
12. Langner, C. A., Birkenmeier, E. H., Roth, K. A., Bronson, R. T., and Gordon, J. I. (1991) *J. Biol. Chem.* **266,** 11955–11964
13. Reue, K., Xu, P., Wang, X. P., and Slavin, B. G. (2000) *J. Lipid Res.* **41,** 1067–1076
14. Nadra, K., de Preux Charles, A. S., Médard, J. J., Hendriks, W. T., Han, G. S., Grès, S., Carman, G. M., Saulnier-Blache, J. S., Verheijen, M. H., and Chrast, R. (2008) *Genes Dev.* **22,** 1647–1661
15. Bou Khalil, M., Sundaram, M., Zhang, H. Y., Links, P. H., Raven, J. F., Manmontri, B., Sariahmetoglu, M., Tran, K., Reue, K., Brindley, D. N., and Yao, Z. (2009) *J. Lipid Res.* **50,** 47–58
16. Chen, Z., Gropler, M. C., Norris, J., Lawrence, J. C., Jr., Harris, T. E., and Finck, B. N. (2008) *Arterioscler. Thromb. Vasc. Biol.* **28,** 1738–1744
17. Zeharia, A., Shaag, A., Houtkooper, R. H., Hindi, T., de Lonlay, P., Erez, G., Hubert, L., Saada, A., de Keyzer, Y., Eshel, G., Vaz, F. M., Pines, O., and Elpeleg, O. (2008) *Am. J. Hum. Genet.* **83,** 489–494
18. El-Shanti, H. I., and Ferguson, P. J. (2007) *Clin. Orthop. Relat. Res.* **462,** 11–19
19. Ferguson, P. J., and El-Shanti, H. I. (2007) *Curr. Opin. Rheumatol.* **19,** 492–498
20. Ferguson, P. J., Chen, S., Tayeh, M. K., Ochoa, L., Leal, S. M., Pelet, A., Munnich, A., Lyonnet, S., Majeed, H. A., and El-Shanti, H. (2005) *J. Med. Genet.* **42,** 551–557
21. Al-Mosawi, Z. S., Al-Saad, K. K., Ijadi-Maghsoodi, R., El-Shanti, H. I., and Ferguson, P. J. (2007) *Arthritis Rheum.* **56,** 960–964
22. Jamal, Z., Martin, A., Gomez-Muñoz, A., and Brindley, D. N. (1991) *J. Biol. Chem.* **266,** 2988–2996
23. Martin, A., Gomez-Muñoz, A., Jamal, Z., and Brindley, D. N. (1991) *Methods Enzymol.* **197,** 553–563
24. Hopewell, R., Martin-Sanz, P., Martin, A., Saxton, J., and Brindley, D. N. (1985) *Biochem. J.* **232,** 485–491
25. Donkor, J., Sparks, L. M., Xie, H., Smith, S. R., and Reue, K. (2008) *J. Clin.*

Endocrinol. Metab. **93,** 233–239
26. Gomez-Muñoz, A., Hatch, G. M., Martin, A., Jamal, Z., Vance, D. E., and Brindley, D. N. (1992) *FEBS Lett.* **301,** 103–106
27. Burroughs, A. M., Allen, K. N., Dunaway-Mariano, D., and Aravind, L. (2006) *J. Mol. Biol.* **361,** 1003–1034
28. Phan, J., and Reue, K. (2005) *Cell Metab.* **1,** 73–83
29. Sciorra, V. A., and Morris, A. J. (2002) *Biochim. Biophys. Acta* **1582,** 45–51
30. Wang, X., Devaiah, S. P., Zhang, W., and Welti, R. (2006) *Prog. Lipid Res.* **45,** 250–278
31. Grkovich, A., and Dennis, E. A. (2009) *Adv. Enzyme Regul.* **49,** 114–120
32. Brindley, D. N., Pilquil, C., Sariahmetoglu, M., and Reue, K. (2009) *Biochim. Biophys. Acta* **1791,** 956–961